The Contributions of Through-Bond Interactions to the Singlet−Triplet Energy Difference in 1,3-Dehydrobenzene

Haiyan Wei,[†] David A. Hrovat,[†] Yirong Mo,[‡] Roald Hoffmann,[§] and Weston Thatcher Borden[†,*]

Department of Chemistry and Center for Advanced Scientific Computing and Modeling, University of North Texas, 1155 Union Circle, #305070, Denton, Texas 76203-5070, Department of Chemistry, Western Michigan University, Kalamazoo, Michigan 49008, and Department of Chemistry and Chemical Biology, Cornell University, Baker Laboratory, Ithaca, New York 14853-1301

Separation of the through-space (TS) from the through-bond (TB) interactions between the two atomic orbitals at C(1) and C(3) of 1,3-dehydrobenzene (**1**) has been achieved by carrying out ab initio, valence-bond, self-consistent-field (VBSCF) calculations. The results indicate that, at the CCSD(T)/cc-pVTZ optimized geometry of the singlet state of **1**, the stabilization provided by TB interactions contributes 10% more than the stabilization provided by the TS interactions to the adiabatic singlet−triplet energy difference. The highest occupied MO of **1** contains a contribution from a hybrid AO at C(2), which has the same phase as the smaller lobes of the AOs at C(1) and C(3). Consequently, TB interactions in **1** increase with decreasing values of the C(1)−C(3) distance. The origin of this hybrid AO at C(2) and the contributions of hyperconjugation to TB and TS interactions in **1** are described and discussed.

Introduction

Singlet 1,3-dehydrobenzene (*m*-benzyne, **1**) has a history that extends over nearly half a century.[1] However, it was not until the 1990s that there was significant progress in the experimental study of **1**. During that decade, measurements were made of (a) the heat of formation of **1**,[2] (b) the singlet−triplet energy difference (ΔE_{S-T}) in **1**,[3] and (c) the IR spectrum of matrix-isolated **1**.[4] These experiments led to a renewed interest in **1** by computational chemists, which still shows no sign of abating.[5]

1   **2**   **3**
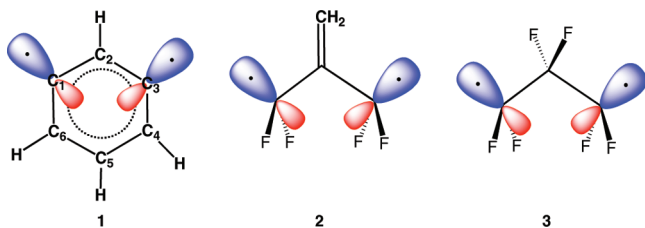
Until 1993, it was generally assumed that a two-configuration wave function, which provides correlation for the two weakly bonding electrons in **1**,[6] should afford an adequate description of the singlet ground state of **1**. However, calculations, published by two different research groups that year,[5a,b] showed that such a wave function underestimates the amount of bonding between C(1) and C(3) and that inclusion of dynamic electron correlation[7] is essential for computing both the heat of formation of and the singlet−triplet splitting in **1**. In order to compute an IR spectrum that is in good agreement with the spectrum obtained for **1** in matrix isolation, a highly correlated wave function must even be used to optimize the C(1)−C(3) bond length.[4b,5j,k]

Despite the very large number of computational studies of **1**,[5] there have been few attempts to ascertain the source of C(1)−C(3) bonding in the singlet state. It seems to have been tacitly assumed that most or all of the bonding comes from direct, through-space (TS) interaction between AOs at these two carbons. However, the possibility of a contribution from through-bond (TB) interactions was raised in a paper published forty years ago. One of us wrote, "The C−H bond [at C(2)] is a most important contributor to the interaction [between C(1) and C(3)], but we do not have an interpretation of its action".[8]

More recently, Winkler and Sander have used both topological and NBO analyses to investigate the electronic structure of **1**.[5j] On the basis of their calculations, they also concluded "The most important delocalization is found to be the donation of electron density from the bonding C(1)−C(3) orbital into the C(2)−H antibond." However, they also added "TB coupling involving the geminal C(1)−C(2) and C(2)−C(3) σ bonds is of similar importance."[5j] Unfortunately, a detailed description of exactly how these bonds mediate the interaction between C(1) and C(3) was not provided.

The recent discovery of the existence of **2**[9] and **3**,[10] the "bond-stretched invertomers" of, respectively, tetrafluoro-methylenecyclopropane and perfluorocyclopropane, has led us to reinvestigate the nature of TS and TB interactions[11] in **1**. Like **1**, bond-stretched invertomers **2** and **3** can be regarded as 1,3-diradicals in which the singlet ground states are stabilized, relative to the triplet excited states, by a combination of TS and TB interactions.

If the interactions between the AOs on C(1) and C(3) in **2** and **3** were strongly mediated by the σ bonds to the substituents at C(2), it seems likely that the differences between the sp^2 C−C σ bond in **2** and the pair of sp^3 C−F σ bonds in **3** would result in very substantial differences between the singlet−triplet energy splittings (ΔE_{S-T}), in these two bond-stretched invertomers. However, the calculated, CASPT2, values of ΔE_{S-T} in **2** and **3** of, respectively, 11.2[10] and 13.8[11] kcal/mol differ by only about

* Corresponding author. E-mail: borden@unt.edu.
† University of North Texas.
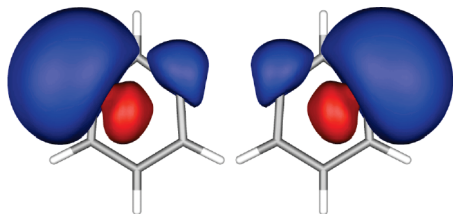‡ Western Michigan University.
§ Cornell University.

Figure 1. Pair of semilocalized VB orbitals for 1,3-dehydrobenzene (**1**), plotted with an isodensity value of 0.015. Only basis functions on C(1) and C(3) were allowed to contribute to each of the VB orbitals. Therefore, TS but not TB interactions between these two carbons is incorporated into the VB wave function.

Figure 2. Pair of fully delocalized GVB orbitals for 1,3-dehydrobenzene (**1**), plotted with an isodensity value of 0.030. Basis functions on all the atoms were allowed to contribute to each of the GVB orbitals, so that both TS and TB interactions were incorporated into the GVB wave function.

25%. Therefore, it would appear that, in **2** and **3**, either (a) TB interactions are dominated by TS interactions or (b) TB interactions between the AOs on C(1) and C(3) are not primarily mediated by the bonds to the substituents that are attached to C(2), in these two diradicals.

As a part of a study of the role and the nature of TS and TB interactions between C(1) and C(3) in stabilizing the singlet states of 1,3-diradicals, such as **2** and **3**, we have carried out valence-bond (VB)[12] calculations on **1**. In this paper, we report the results of these calculations. We have found that at some geometries TB interactions actually do play a larger role than TS interactions in adiabatically stabilizing the singlet ground state of **1**, relative to the lowest triplet. In order to probe the nature of the TB interactions in **1**, calculations on several model compounds have also been performed.

Computational Methodology

We carried out calculations with the recently developed XMVB method.[13] We chose this method because it enabled us to calculate the energies of a VB wave function for **1** that contains only TS interactions between ϕ_1 and ϕ_3, the nonbonding AOs that are located at, respectively, C(1) and C(3). Localization of a pair of electrons in just these two AOs was achieved by allowing only basis functions on these two carbons to contribute to the VB orbitals for this pair of electrons.

The VB orbitals for this pair of electrons are shown in Figure 1. One of these electrons is localized more in ϕ_1 than in ϕ_3, whereas the reverse is true for the other electron. By partially localizing this pair of electrons to different regions of space, the VB wave function strikes the optimal balance between maximization of TS bonding between ϕ_1 and ϕ_3 and minimization of the Coulombic repulsion between the pair of opposite spin electrons that occupy these two AOs in the singlet ground state.

VB calculations were also performed in which basis functions on all the atoms of **1** were allowed to contribute to the VB orbitals, thus allowing the pair of partially localized electrons in the first type of VB wave function to become fully delocalized. Thus, not only TS but also TB interactions between the AOs on C(1) and C(3) were included in the fully delocalized VB wave function.

For calculations in which the VB wave function was allowed to be fully delocalized, generalized (G)VB calculations,[14] performed with Gaussian 03,[15] provide an attractive alternative to VB calculations, carried out with the XMVB program.[13] Both methods give the same electronic energies; but the GVB calculations, performed with Gaussian 03, have the following three advantages over VB calculations performed with the XMVB program: (a) the singly and doubly occupied VB orbitals are not necessarily orthogonal to each other, whereas the singly and doubly occupied GVB orbitals are, (b) analytical geometry
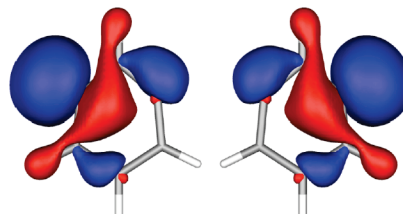
optimizations cannot be performed with the XMVB program, and (c) the XMVB program cannot currently handle very large basis sets.

Therefore, wave functions that were allowed to be fully delocalized were obtained with GVB calculations, and Gaussian 03 was used to optimize the GVB geometries. Consequently, in this paper, VB is used to designate calculations performed with a pair of VB orbitals that, like those in Figure 1, were constrained to be localized at C(1) and C(3); and GVB is used for calculations in which this pair of orbitals was allowed to be fully delocalized, like the GVB orbitals shown in Figure 2.

In classical VB theory, the delocalization energy is obtained by calculating the energy difference between partially localized and fully delocalized VB wave functions.[12] In our calculations on **1**, $^1E(TB)$, the interaction energy of the AOs on C(1) and C(3) with the σ bonds of **1** in the singlet ground state, is taken to be the difference between the energies of the partially localized VB singlet and the fully delocalized GVB singlet wave functions at the same geometry.

$$^1E(TB) = {}^1E(VB) - {}^1E(GVB) \qquad (1)$$

Although GVB is only used in this paper to denote singlet wave functions, we have put a superscript 1 on $E(GVB)$ in eq 1 for the sake of consistency and clarity.

The triplet equivalent of a singlet GVB wave function is a restricted, open-shell, (RO)HF, triplet wave function.[16] Therefore, $^3E(TB)$, the interaction energy of the AOs on C(1) and C(3) with the σ bonds in the triplet state of **1**, is taken to be the difference between the energies of the partially localized VB triplet and fully delocalized ROHF triplet wave functions. Thus,

$$^3E(TB) = {}^3E(VB) - {}^3E(ROHF) \qquad (2)$$

The contribution of TB interactions to the ROHF/GVB singlet−triplet energy difference is then given by

$$\Delta E_{S\text{-}T}(TB) = {}^1E(TB) - {}^3E(TB) \qquad (3)$$

$$= {}^1E(VB) - {}^1E(GVB) - {}^3E(VB) + {}^3E(ROHF) \qquad (4)$$

$$= \Delta E_{S\text{-}T}(ROHF/GVB) - \Delta E_{S\text{-}T}(VB) \qquad (5)$$

Equation 5 shows that the contribution of TB interactions to the ROHF/GVB singlet−triplet energy splitting is equal to the difference between the S−T energy splittings, computed with

Contributions of TB Interactions to $\Delta E_{\text{S}-\text{T}}$ in 1,3-Dehydrobenzene

J. Phys. Chem. A, Vol. 113, No. 38, 2009 **10353**

the fully delocalized ROHF/GVB wave functions and with the partially localized triplet and singlet VB wave functions.

Equations 4 and 5 are only valid if the VB and ROHF triplet energies are both evaluated at the same geometry and if the VB and GVB singlet energies are also both evaluated at the same geometry. However, the singlet and triplet energies in eqs 4 and 5 can be obtained at different geometries. Therefore, these equations can be used to compute the contribution of TB interactions to adiabatic, as well as to vertical singlet−triplet energy differences.

An expression for the contribution of TS interactions to the ROHF/GVB singlet−triplet energy difference can be obtained by combining eq 5 with the definition.

$$\Delta E_{\text{S-T}}(\text{ROHF/GVB}) = \Delta E_{\text{S-T}}(\text{TS}) + \Delta E_{\text{S-T}}(\text{TB}) \quad (6)$$

Substituting $\Delta E_{\text{S}-\text{T}}(\text{TB})$ from eq 5 in eq 6 and rearranging gives

$$\Delta E_{\text{S-T}}(\text{TS}) = \Delta E_{\text{S-T}}(\text{VB}) \quad (7)$$

If $\Delta E_{\text{S}-\text{T}}'(\text{TS})$ in eq 7 is computed as the difference between $^3E(\text{VB})$ at the equilibrium geometry of the triplet and $^1E(\text{VB})$ at the equilibrium geometry of the singlet, the resulting value of $\Delta E_{\text{S}-\text{T}}(\text{TS})$ is the contribution of TS interactions to the adiabatic energy difference between the ROHF triplet and GVB singlet.

The concepts of TS and TB interactions between AOs were originally formulated[8] and still are usually discussed within the context of MO rather than VB theory.[11] Therefore, it is appropriate to describe how the partially localized VB and fully delocalized GVB wave functions for **1** can be represented by equivalent MO wave functions, written in terms of the symmetric (S) and antisymmetric (A) combinations of ϕ_1, ϕ_3 and the AOs that interact with them.

$$\psi_{\text{S}} = (\varphi_1 + \varphi_3)/\sqrt{2} \quad (8)$$

$$\psi_{\text{A}} = (\varphi_1 - \varphi_3)/\sqrt{2} \quad (9)$$

The partially delocalized, singlet, VB wave function for **1**, with a pair of electrons allowed to be delocalized only between ϕ_1 and ϕ_3, is

$$^1\psi(\text{VB}) = |...(c_1\varphi_1 + c_3\varphi_3)(c_3\varphi_1 + c_1\varphi_3)(\alpha\beta - \beta\alpha)>/\sqrt{2} \quad (10)$$

where $c_1\phi_1 + c_3\phi_3$ is the partially delocalized VB orbital for one electron and $c_3\phi_1 + c_1\phi_3$ is the partially delocalized VB orbital for the other. As already noted in connection with the VB orbitals that are pictured in Figure 1, by partially localizing the pair of electrons that occupy these orbitals to different regions of space, the VB wave function strikes the optimal balance between maximization of TS bonding between ϕ_1 and ϕ_3 and minimization of the Coulombic repulsion between the pair of opposite-spin electrons that occupy these two AOs in the lowest singlet state.

As shown in the Supporting Information,[17] $^1\Psi(\text{VB})$ can be rewritten in terms of the sum and difference of the two, semidelocalized, VB orbitals in eq 10. This allows $^1\Psi(\text{VB})$ to

be expressed in terms of the symmetric and antisymmetric combinations of ϕ_1 and ϕ_3 in eqs 8 and 9 as a two-configuration (TC)SCF wave function

$$^1\psi(\text{VB}) = [(c_1 + c_3)^2|...\psi_{\text{S}}^2 > -(c_1 - c_3)^2|...\psi_{\text{A}}^2>]/2 \quad (11)$$

where c_1 and c_3 have the same values in both eqs 10 and 11.

Because Ψ_{S} is the in-phase,TS-bonding combination of ϕ_1 and ϕ_3, it is lower in energy than Ψ_{A}, which is the out-of-phase, TS-antibonding combination. Therefore, the first configuration contributes more than the second to eq 11. Consequently, if $c_1 > 0$, then $c_3 > 0$ in eq 11 and also, of course, in eq 10.

In the singlet GVB wave function, $^1\Psi(\text{GVB})$, for **1**, each of the partially localized VB orbitals in eq 10 is now allowed to be delocalized over all the σ AOs rather than being confined to just ϕ_1 and ϕ_3, as in $^1\Psi(\text{VB})$. An equivalent TCSCF wave function, $^1\Psi(\text{TCSCF})'$, can be written for $^1\Psi(\text{GVB})$ in terms of the sum and difference of the GVB orbitals.[16] The TCSCF version of $^1\Psi(\text{GVB})$ is

$$^1\psi(\text{GVB}) = {}^1\psi(\text{TCSCF}) = [c_{\text{S}}^2|...\psi_{\text{S}}'^2 > -c_{\text{A}}^2|...\psi_{\text{A}}'^2>]/\sqrt{2} \quad (12)$$

where Ψ_{S}' and Ψ_{A}' are each allowed to be delocalized over combinations of all the σ AOs that have the correct symmetry rather than being confined just to ϕ_1 and ϕ_3, as Ψ_{S} and Ψ_{A} are in eqs 8 and 9.

Singlet and triplet VB calculations on **1** were both carried out with the XMVB program.[13,18] The VB calculations on the lowest singlet and triplet states of **1** were performed at geometries that had been optimized with, respectively, ^{1}GVB (TCSCF) and ^{3}ROHF calculations, using the 6-31G(d) basis set.[19] Geometry optimizations were carried out with the Gaussian03 package of programs.[15]

The inclusion of dynamic electron correlation in the wave function for singlet **1** strengthens the bonding between C(1) and C(3),[5,7] which helps overcome some of the strain that is associated with distorting the bond angles in *meta*-benzyne from the idealized benzenoid value of 120°. Consequently, the CCSD(T)/6-31G(d,p) value of $R_{13} = 2.107$ Å[4a] [(C(1)−C(2)−C(3) = 99.8°)] is nearly 0.1 Å shorter than the ^{1}GVB/6-31G(d) value of $R_{13} = 2.198$ Å [(C(1)−C(2)−C(3) = 106.5°)]. CCSD(T) calculations with the cc-pVTZ basis set give an even smaller value of $R_{13} = 2.026$ Å [(C(1)−C(2)−C(3) = 95.9°)], and Crawford and co-workers have conjectured that the CCSDT/cc-pVTZ value is $R_{13} = 2.013$ Å.[5j]

On the basis of the results of Crawford and co-workers, a value of R_{13} in singlet **1** that is closer to 2.0 Å seems much more likely than one that is close to the GVB/6-31G(d) value of 2.198 Å. However, in order to determine how the TS and TB interactions in **1** depend on R_{13}, we carried out singlet VB and GVB calculations at the GVB/6-31G(d), CCSD(T)/6-31G(d,p), and CCSD(T)/cc-pVTZ optimized geometries for the singlet. We also performed triplet VB and ROHF calculations at the ROHF/6-31G(d) and CCSD(T)/6-31G(d,p) optimized geometries for the triplet.

In order to include the effects of dynamic electron correlation[7] in our ^{1}GVB and ^{3}ROHF calculations, CASPT2/6-31G(d) calculations[20] were performed at the GVB, ROHF/6-31G(d), CCSD(T)/6-31G(d,p), and CCSD(T)/cc-pVTZ optimized geometries for the singlet and triplet. The single-point CASPT2 calculations were all carried out with MOLCAS.[21]
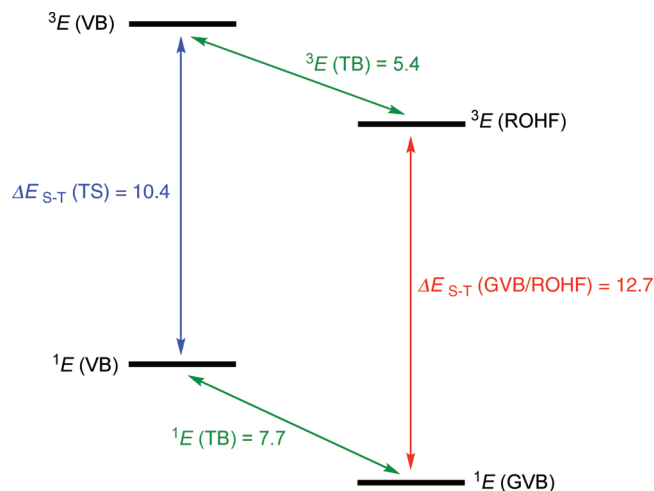
Figure 3. Results of triplet and singlet VB, triplet ROHF, and singlet GVB calculations on **1** with the 6-31G(d) basis set at ROHF and GVB/6-31G(d) optimized geometries. Energy differences are adiabatic and are given in kcal/mol. A Figure showing the relationship between the adiabatic and the vertical energy differences at the GVB/6-31G(d) optimized geometry is available in the Supporting Information.[17]

TABLE 1: Adiabatic Values of ΔE_{S-T}(TS), ΔE_{S-T}(TB), ΔE_{S-T}(GVB/ROHF), and ΔE_{S-T}(CASPT2) (in kcal/mol), Calculated with the 6-31G(d) Basis Set, at the C(1)—C(3) Bond Lengths (R_{13}, Å) in the GVB/6-31G(d), CCSD(T)/6-31G(d,p), and CCSD(T)/cc-pVTZ Optimized Geometries of Singlet 1[a]

R_{13}	ΔE_{S-T} (TS)	ΔE_{S-T} (TB)	ΔE_{S-T} (ROHF/GVB)	ΔE_{S-T} (CASPT2)
2.198[b]	10.4	2.3	12.7	20.2
2.107[c]	7.4	3.7	11.1	21.3
2.026[d]	4.7	5.2	9.9[e]	20.9[f]

[a] Geometries of the triplets were optimized at the same levels of theory as the geometries of the correponding singlets. [b] GVB/6-31G(d) optimized geometry. [c] CCSD(T)/6-31G(d,p) optimized geometry. [d] CCSD(T)/cc-pVTZ optimized geometry. [e] At the CCSD(T)/cc-pVTZ optimized singlet geometry, the vertical value of ΔE_{S-T}(GVB/ROHF) = 34.5 kcal/mol that was obtained with the 6-31G(d) basis set was only 0.02 kcal/mol higher than the value computed with the cc-pVTZ basis set. [f] The CCSD(T)/6-31G(d,p) triplet geometry was used for this calculation.

Results and Discussion

Results of VB, GVB, and ROHF Calculations. The results of our ³VB, ¹VB, ³ROHF, and ¹GVB calculations at the ROHF and GVB optimized geometries of **1** are summarized in Figure 3. TS interactions between ϕ_1 and ϕ_3 contribute ΔE_{S-T}(TS) = 10.4 kcal/mol to the adiabatic singlet−triplet energy difference of ΔE_{S-T}(GVB/ROHF) = 12.7 kcal/mol.[22] At the ROHF and GVB geometries, the contribution of TS interactions between C(1) and C(3) to the adiabatic singlet−triplet energy difference is more than a factor of 4 larger than the contribution of the difference between the adiabatic TB interactions in the singlet and triplet, for which ΔE_{S-T}(TB) = 7.7 − 5.4 = 2.3 kcal/mol.

Table 1 shows how the adiabatic values of ΔE_{S-T}(TS), ΔE_{S-T}(TB), ΔE_{S-T}(GVB/ROHF), and ΔE_{S-T}(CASPT2) change at values of R_{13} in the singlet that are shorter than the value of R_{13} = 2.198 Å at the GVB/6-31G(d) optimized geometry. The adiabatic singlet−triplet energy difference, ΔE_{S-T}(GVB/ROHF), decreases as R_{13} shortens, because the adiabatic TS contribution, ΔE_{S-T}(TS), decreases in size by more than the adiabatic TB contribution, ΔE_{S-T}(TB), increases.
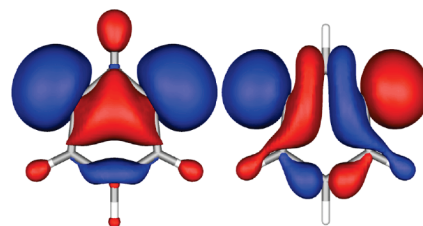

Figure 4. TCSCF orbitals, ψ_S' and ψ_A' of **1** plotted with an isodensity value of 0.030. The TCSCF MOs are, respectively, the sum and difference of the GVB orbitals in Figure 2.

The opposite signs of the changes in ΔE_{S-T}(TS) and ΔE_{S-T}(TB) mean that, as R_{13} shortens, the contributions of TB interactions to ΔE_{S-T}(GVB/ROHF) grow in importance, relative to the contributions of TS interactions. In fact, at R_{13} = 2.026 Å, TB interactions actually make a contribution 10% larger than that of TS interactions to the adiabatic value of ΔE_{S-T}(GVB/ROHF) = 9.9 kcal/mol.[23] The increase in ΔE_{S-T}(TB) with decreasing C(1)—C(3) distance also means that TB interactions cause the equilibrium geometry of the singlet state of **1** to occur at a shorter value of R_{13} than if only TS bonding interactions controlled the equilibrium C(1)—C(3) bond length.

Inclusion of the Effects of Dynamic Electron Correlation. Table 1 shows that inclusion of dynamic electron correlation at the CASPT2 level has two effects. First, the adiabatic values of ΔE_{S-T}(CASPT2) are 60−110% larger than the adiabatic values of ΔE_{S-T}(GVB/ROHF) and in much better agreement with the experimental value of ΔE_{S-T} = 21.0 kcal/mol.[3] Second, like the CCSD(T) singlet energy minimum,[4b,5i,j] the CASPT2 singlet energy minimum appears to occur at a shorter value of R_{13} than the GVB singlet energy minimum, thus indicating that TB interactions probably play a more important role in the value of ΔE_{S-T} that is computed at the CASPT2 than at the GVB optimized geometry.

Breathing orbital (BO)VB calculations[24] could, in principle, be used to deconvolute into TS and TB contributions the effect of dynamic electron correlation on ΔE_{S-T} in **1**. Unfortunately, using the XMVB program,[12,18] we were unable to converge BOVB calculations on **1**.

Evidence that dynamic electron correlation enhances TB, as well as TS interactions, comes from calculations on 1,4-dehydrobenzene. In this diradical, TB and TS interactions involve orbitals of different symmetry, and the former interactions dominate the latter.[8] Inclusion of dynamic correlation more than doubles the calculated size of the singlet−triplet gap in 1,4-dehydrobenzene, from less than 1 kcal/mol to 2−4 kcal/mol.[25]

The Origin of the TB Interactions in 1. What is the nature of these TB interactions which favor shorter C(1)—C(3) bond lengths in **1** and selectively stabilize the singlet state? The answer to this question can be gleaned from comparisons of the partially delocalized VB and fully delocalized GVB orbitals in Figures 1 and 2 and from inspection of the TCSCF MOs, ψ_S' and ψ_A', in Figure 4.

Careful inspection of Figure 1 shows that, in each of the VB orbitals, the AO on C(1) has a slightly different spatial orientation than the AO on C(3). We will defer for a moment the explanation of why the orientation of the AO that is the smaller contributor to each of the VB orbitals differs from the orientation of the AO that is the larger contributor.

The changes that occur when going from the VB orbitals in Figure 1 to the GVB orbitals in Figure 2 reveal which AOs on other atoms are responsible for the TB interactions between the

Contributions of TB Interactions to ΔE_{S-T} in 1,3-Dehydrobenzene

J. Phys. Chem. A, Vol. 113, No. 38, 2009 **10355**

AOs at C(1) and C(3). For example, in the GVB orbital on the left-hand side of Figure 2, the VB orbital on the left-hand side of Figure 1 becomes delocalized into AOs on C(2) and C(6) that overlap in a bonding fashion with the smaller of the two lobes of ϕ_1. The smaller lobe of the hybrid AO on C(2) also interacts in a bonding fashion with the larger lobe of the AO at C(3). In addition, an AO on C(5) and the 1s AOs of the hydrogens that are attached to C_2 and C_6 contribute to this GVB orbital. Of course, analogous delocalization occurs when going from the VB orbital on the right-hand side of Figure 1 to the GVB orbital on the right-hand side of Figure 2.

The TCSCF orbitals, ψ_S' and ψ_A', of **1** are shown in Figure 4. Winkler and Sander have suggested that the TB interactions between C(1) and C(3) have their origin in a σ allylic C(1)–C(2)–C(3) system.[5i] This is a very good description of the combinations of the AOs at these three carbons in ψ_S' and ψ_A' in Figure 4.

In the ψ_S' TCSCF MO, the AO on C(2) that results from adding the two GVB orbitals in Figure 2 is hybridized toward the center of the benzene ring, so that it is favorably oriented for interacting in a bonding way with the smaller lobes of the AOs at C(1) and C(3). Because the AO on C(2) in ψ_S' is hybridized away from the hydrogen that is attached to this carbon, this hybrid AO on C(2) does not appear to be associated primarily with the C(2)–H bond. Instead, this hybrid AO comes from the in-phase combination of AOs on C(2) that are associated with bonding interactions between C(2) and C(1) in one GVB orbital and between C(2) and C(3) in the other.

In the ψ_A' TCSCF MO in Figure 4, the AO on C(2), which comes from the out-of-phase combination of the GVB orbitals, is a pure 2p AO that is oriented tangentially, rather than radially, with respect to the benzene ring. Consequently, although the overlap of this AO with the smaller lobes of ϕ_1 and ϕ_3 is bonding, this AO on C(2) interacts more strongly in an antibonding fashion with the larger lobes of ϕ_1 and ϕ_3. It is, in fact, the difference between the ways that an AO on C(2) interacts with the AOs on C(1) and C(3) in ψ_S' and ψ_A' that is chiefly responsible for the TB contribution to the energy difference between the symmetric and antisymmetric TCSCF MOs.

The energy difference between Ψ_S' and Ψ_A' plays an important role in ΔE_{S-T}. In the TCSCF expression for ${}^1\Psi(\text{GVB})$ in eq 12, $c_S{}^2 = 0.88$ and $c_A{}^2 = 0.47$ at the optimized geometry of singlet **1**, which makes the occupation numbers of Ψ_S' and Ψ_A' 1.56 and 0.44 electrons, respectively. In contrast, in $\Psi(\text{ROHF})$ for the triplet, the occupation numbers of Ψ_S' and Ψ_A' are each 1.00. The greater occupation number of Ψ_S' and the smaller occupation number of Ψ_A' in the singlet than in the triplet are responsible for the lower energy of the singlet.

Three Models for the TB Interactions in 1. Why do AOs on C(2) appear in the GVB orbitals in Figure 2 and, hence, in the ψ_S' and ψ_A' TCSCF MOs in Figure 4? In order to address this question, we performed a calculation on phenyl radical (**4**), so that we could compare the AOs on atoms, other than C(1), that contribute to the SOMO of **4** with the AOs that appear in each of the GVB orbitals of **1** in Figure 2.

Comparison of Figure 5a with Figure 2 shows that AOs on C(2) and C(6) contribute to the SOMO of **4** in the same way that the AOs on the corresponding atoms of **1** contribute to each of the pair of GVB orbitals for it. The AOs on C(2) and C(6) of **4**, which are largely directed along the bonds to C(1) and hybridized toward this carbon, overlap the smaller lobe of ϕ_1 in a bonding fashion. The AOs on C(3) and C(5) of **4** lie along
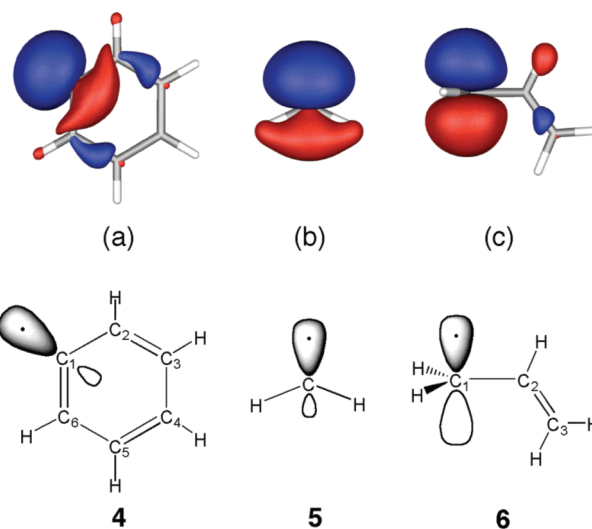

Figure 5. σ SOMOs of (a) phenyl radical (**4**), (b) triplet methylene (**5**), and (c) an allyl radical (**6**), but with the radical center at C(1) twisted out of conjugation and constrained to be locally planar. The orbital plots were made with an isodensity value of 0.015.

the bonds to, respectively, C(2) and C(6) and overlap the smaller lobe of ϕ_1 in an antibonding fashion.

The phasing of the AOs on C(2) and C(3) and on C(5) and C(6), relative to ϕ_1, results in the AOs on C(2) and C(3) and on C(5) and C(6) overlapping in a bonding fashion in the SOMO of **4**. However, the difference in the spatial orientations of these pairs of AOs in the SOMO of **4** reduces the overlap between them and thus diminishes the contribution of the bonding interaction between them to the C(2)–C(3) and C(5)–C(6) bonds of **4**.

In the SOMO of **4**, the interactions of the larger lobe of ϕ_1 with the 1s AOs of the hydrogens that are attached to C(2) and C(6), are, like the interactions of the smaller lobe of ϕ_1 with the AOs on C(3) and C(5), antibonding. Thus, although the AOs on C(2) and C(6) interact with ϕ_1 in a bonding fashion in the SOMO of **4**, the AOs on all of the atoms that are attached to these two carbons interact with ϕ_1 in an antibonding fashion.

In order to better understand the very similar types of AO interactions in the GVB orbitals of **1** and in the SOMO of **4**, we carried out ROHF calculations on triplet methylene (**5**) and on allyl radical (**6**), but with the radical center at C(1) in **6** twisted out of conjugation and constrained to be locally planar. The σ SOMOs of **5** and **6** are shown, respectively, in panels b and c of Figure 5.

Because **5** has only a pair of hydrogens attached directly to the radical center, there is no possibility of hyperconjugation in **5**. Therefore, the bonding between the hydrogen 1s AOs and the smaller lobe of the singly occupied AO on carbon in **5** must have another origin. In fact, the contribution of the hydrogens to the σ SOMO of **5** are a feature of the in-plane, weakly bonding, $3a_1$ MOs in all bent AH_2 molecules in the first row of the periodic table, ranging from $BH_2\bullet$ to H_2O and H_2F^+.[26]

The contributions of the AOs at C(2) and C(6) to the GVB orbital of **1** in the left-hand side of Figure 2 and to the SOMO of **4** in Figure 5a have exactly the same origin. The only difference is that, in place of the 1s AOs on hydrogen in **5**, in **1** and **4**, hybrid AOs at C(2) and C(6) are directed toward the smaller lobe of the AO at C(1).

As discussed in the preceding section, it is the contribution of a hybrid AO at C(2) to each of the GVB orbitals of **1** in Figure 2 that makes the interaction between C(2) and ϕ_1 and ϕ_3

more bonding in ψ_S' than in ψ_A'. In the ψ_S' TCSCF MO, which is the sum of the GVB orbitals, the C(2) AO in the GVB orbital on the left-hand side of Figure 2 interacts in a bonding fashion with ϕ_3 in the GVB orbital on the right-hand side of Figure 2, and the C(2) AO in the GVB orbital on the right-hand side of Figure 2 interacts in a bonding fashion with ϕ_1 in the GVB orbital on the left-hand side of Figure 2.

As already noted, adding the AOs on C(2) in the pair of GVB orbitals in Figure 2 gives the AO on C(2) that is hybridized toward the center of the benzene ring in ψ_S' of Figure 4. Therefore, it would be correct to say that the major source of TB contributions to the energy difference between ψ_S and ψ_A (and, hence, to ΔE_{S-T}) in **1**, has the same origin as the contribution of the 1s AOs on hydrogen to the σ SOMO of triplet methylene (**5**) in Figure 5b.[26]

The AO at C(1) in the SOMO of **6**, which is shown in Figure 5c, is a pure 2p AO that is orthogonal to the C(1)—C(2) σ bond. Therefore, hyperconjugation with the other bonds to C(2) is the only mechanism by which this 2p AO on C(1) can interact with C(2). In fact, as shown in Figure 5c, the hyperconjugative interactions in the SOMO of **6**, like those in the GVB orbitals of **1** and in the SOMO of **4**, do not lead to a significant contribution from AOs on the carbon that is attached to the radical center. Instead, it is AOs on the atoms that are bonded to C(3) of **6** that contribute to the SOMO, and these AOs contribute with a phase that is opposite to the phase of the 2p AO at the radical center.[27]

The effect of hyperconjugation on the GVB orbitals of **1** and on the SOMO of **4** is exactly the same as in the SOMO of **6**. Hyperconjugation is not responsible for much, if any, of the contributions of AOs on C(2), C(4), and C(6) to either of the GVB orbitals of **1** or to the SOMO of **4**. However, hyperconjugation does lead to contributions of AOs on C(3) and C(5) to the SOMO of **4** and to the GVB orbital of **1** that is centered on C(1) and shown on the left-hand side of Figure 2. Hyperconjugation also results in hybrid AOs on C(1) and C(5) contributing to the GVB orbital of **1** that is centered on C(3) and shown on the right-hand side of Figure 2.

As shown in Figure 5a, in the SOMO of **4**, the hybrid AOs at C(3) and C(5) are parallel to the singly occupied AO at the radical center, and these hybrid AOs each have a phase that is opposite to the smaller of the two lobes of the AO at the radical center. This is also the case for the analogous AOs that contribute to each of the GVB orbitals of **1** in Figure 2.

Thus, there are really two different AOs at C(3) which contribute to the GVB orbital that is shown on the left side of Figure 2 and is comprised largely of ϕ_1 on C(1). The presence of ϕ_3 in this GVB orbital is due to the TS interaction of ϕ_1 with ϕ_3. The presence of the other AO on C(3) in this GVB orbital is due to a hyperconjugative interaction of ϕ_1 with the σ and σ^* orbitals of the C(2)—C(3) bond. As shown schematically in Figure 6, these two AOs at C(3) give a GVB orbital in which the resultant AO at C(3) is rotated, so that it lies closer than ϕ_3 to the C(3)—C(4) bond. Similarly, in the other GVB orbital in Figure 2, mixing of the two AOs at C(1), which results from (a) TS and (b) hyperconjugative interactions with ϕ_3, gives a hybrid AO at C(1) that is rotated more toward the C(1)—C(6) bond than ϕ_1 is.

It is easy to show mathematically that the rotations of the AOs at C(3) and C(1), which make small contributions to the GVB orbitals in Figure 2, have opposite effects on the TCSCF symmetry orbitals, ψ_S' and ψ_A'.[28] In ψ_S', the rotated AOs at C(1) and C(3) add to ϕ_1 and ϕ_3, whereas, in ψ_A', the rotated AOs subtract from ϕ_1 and ϕ_3. As a result, the AOs at C(1) and
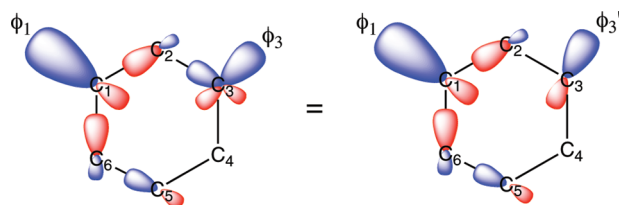

Figure 6. Schematic depiction of the AOs that make major contributions to the GVB orbital of **1** that is comprised largely of ϕ_1 on C(1). ϕ_3 at C(3) interacts through space with ϕ_1. The AOs at C(2) and C(6) that interact with the smaller lobe of ϕ_1 are analogous to the 1s AOs on H that are found in the $3a_1$ MO of any bent AH$_2$ molecule. The AOs at C(3) and C(5) that are parallel to the AO at C(1) come from hyperconjugative interactions of ϕ_1 with the C(2)—C(3) and C(5)—C(6) σ and σ^* bonds. The two AOs at C(3) mix to give a resultant AO, ϕ_3', that is rotated more toward C(1) than ϕ_3 is.

C(3) in Figure 4 can be seen to be rotated more toward the C(2)—H bond in ψ_S' than they are in ψ_A'. Consequently, the smaller of the two lobes of the AOs at C(1) and C(3) interact with each other less strongly in ψ_S' than in ψ_A'. Therefore, hyperconjugative interactions affect the energy difference between ψ_S' and ψ_A' and, hence, the size of ΔE_{S-T} in **1**.

These hyperconjugative contributions to ψ_S', ψ_A', and ΔE_{S-T} involve the C(2)—C(3) and C(5)—C(6) bonds of **1**. Therefore, it might seem correct to conclude that these contributions are TB effects. However, the interaction between the AOs on C(1) and C(3) that are modified by hyperconjugation is a TS effect. Indeed, the rotated AOs at C(1) and C(3) appear in the VB orbitals in Figure 1. Therefore, because part of the contribution of hyperconjugation to the energy difference between ψ_S' and ψ_A' appears in the VB orbitals, this part must be attributed to a TS rather than to a TB interaction.

Conclusions

VB calculations have allowed us to separate the contributions of TS and TB interactions to the adiabatic energy difference between the singlet and triplet states of **1**. TB interactions selectively stabilize the symmetric TCSCF MO (Ψ_S'), and these interactions increase in size as the C(1)—C(3) distance (R_{13}) decreases.[29] Consequently, TB interactions have the effect of both shortening the C(1)—C(3) equilibrium bond length and contributing more to the adiabatic singlet—triplet splitting at geometries of singlet **1** that are optimized with inclusion of dynamic electron correlation.

The TB interactions that are principally responsible for stabilizing Ψ_S' in **1** involve an AO on C(2) that is hybridized toward the center of the benzene ring in the Ψ_S' TCSCF MO. This hybrid AO on C(2) interacts in a bonding fashion with the smaller lobes of the AOs, ϕ_1 and ϕ_3, on C(1) and C(3).

This hybrid does not come principally from the C(2)—H bond[30] but, instead, from the bonds between C(2) and C(1) in one GVB orbital and between C(2) and C(3) in the other. Similar bonds contribute to the σ SOMOs of phenyl radical (**4**), triplet methylene (**5**), and to the weakly bonding, $3a_1$ MOs in all bent AH$_2$ molecules in the first row of the periodic table.[26]

In Ψ_S', the in-phase combination of the GVB orbitals of **1,** the C(2)—C(1) bond in one GVB orbital interacts in a bonding fashion with ϕ_3 in the other GVB orbital, and the C(2)—C(3) bond in the second GVB orbital interacts in a bonding fashion with ϕ_1 in the first. The in-phase combination of the C(2)—C(1) and C(2)—C(3) bonds is what gives rise to the hybrid orbital at C(2) in Ψ_S'.

From the foregoing analysis of the origin of the TB interactions in **1**, we can predict that the size of the TB

Contributions of TB Interactions to ΔE_{S-T} in 1,3-Dehydrobenzene

J. Phys. Chem. A, Vol. 113, No. 38, 2009 **10357**

interactions in a 1,3-diradical should decrease with increasing bond angles at the radical centers. As these bond angles approach 180°, the contributions of the C(1)—C(2) and C(2)—C(3) bonds to Ψ_S' vanish, and it is the presence of these bonds in Ψ_S' that gives rise to the TB interactions in **1**. Therefore, the contribution of TB interactions to the energy of a 1,3-diradical should depend on the extent to which the bond angles at the radical centers deviate from 180°.

This prediction will be tested in our future computational studies of TB and TS interactions in 1,3-diradicals, such as bond-stretched invertomers **2** and **3**, 1,3-dehydroannulenes that are related to **1**, and heteroatom derivatives of **1**–**3**.

Supporting Information Available: TCSCF, ROHF, and CCSD(T) optimized geometries, absolute VB, GVB (= TCSCF), ROHF, CASPT2, and CCSD(T) energies computed at them, derivation of eq 11 from eq 10, a figure that shows the relationship between the adiabatic and vertical energy differences, and the complete list of authors for ref 15 (8 pages). See any current masthead page for ordering information and Web access instructions. This information is available free of charge via the Internet at http://pubs.acs.org.

References and Notes

(1) Reviews: (a) Sander, W. *Acc. Chem. Res.* **1999**, *32*, 669. (b) Sander, W. *Angew. Chem., Int. Ed.* **2003**, *42*, 502.

(2) (a) Wenthold, P. G.; Paulino, J. A.; Squires, R. R. *J. Am. Chem. Soc.* **1991**, *113*, 7414. (b) Wenthold, P. G.; Squires, R. R. *J. Am. Chem. Soc.* **1994**, *116*, 6961. (c) Wenthold, P. G.; Squires, R. R. *J. Am. Chem. Soc.* **1996**, *118*, 11865.

(3) Wenthold, P. G.; Squires, R. R.; Lineberger, W. C. *J. Am. Chem. Soc.* **1998**, *120*, 5279.

(4) (a) Marquardt, R.; Sander, W.; Kraka, E. *Angew. Chem., Int. Ed.* **1996**, *108*, 825. (b) Sander, W.; Exner, M.; Winkler, M.; Balster, A.; Hjerpe, A.; Kraka, E.; Cremer, D. *J. Am. Chem. Soc.* **2002**, *124*, 13072.

(5) (a) Nicolaides, A.; Borden, W. T. *J. Am. Chem. Soc.* **1993**, *115*, 11951. (b) Wiersche, S. G.; Nash, J. J.; Squires, R. R. *J. Am. Chem. Soc.* **1993**, *115*, 11958. (c) Kraka, E.; Cremer, D. *Chem. Phys. Lett.* **1993**, *216*, 333. (d) Kraka, E.; Cremer, D. *J. Am. Chem. Soc.* **1994**, *116*, 4929. (e) Lindh, R.; Persson, B. J. *J. Am. Chem. Soc.* **1994**, *116*, 4963. (f) Lindh, R.; Lee, T. J.; Bernhardsson, B. J.; Persson, B. J.; Karlström, G. *J. Am. Chem. Soc.* **1995**, *117*, 7186. (g) Nash, J. J.; Squires, R. R. *J. Am. Chem. Soc.* **1996**, *118*, 11872. (h) Cramer, C. J.; Nash, J. J.; Squires, R. R. *Chem. Phys. Lett.* **1997**, *277*, 311. (i) de Visser, S. P.; Filatov, M.; Shaik, S. *Phys. Chem. Chem. Phys.* **2000**, *2*, 5046. (j) Winkler, M.; Sander, W. *J. Phys. Chem.* **2001**, *105*, 10422. (k) Smith, C. E.; Crawford, T. D.; Cremer, D. *J. Chem. Phys.* **2005**, *122*, 174309. (l) Evangelista, F. A.; Allen, W. D.; Schaefer, H. F., III. *J. Chem. Phys.* **2007**, *127*, 24102. (m) Li, H.; Yu, S.-Y.; Huang, M.-B.; Wang, Z.-X. *Chem. Phys. Lett.* **2007**, *450*, 12. (n) Shen, J.; Fang, T.; Hua, W.; Li, S. *J. Phys. Chem. A* **2008**, *112*, 4703. (o) Al-Saidi, W. A.; Umrigar, C. J. *J. Chem. Phys.* **2008**, *128*, 154324. (p) Li, X.; Paldus, J. *J. Chem. Phys.* **2008**, *129*, 174101. (q) Karton, A.; Kaminker, I.; Martin, J. M. L. *J. Phys. Chem. A* **2009**, *113*, 7610.

(6) Noell, J. O.; Newton, M. D. *J. Am. Chem. Soc.* **1979**, *101*, 51.

(7) Borden, W. T.; Davidson, E. R. *Acc. Chem. Res.* **1996**, *29*, 87.

(8) Hoffmann, R.; Imamura, A.; Hehre, W. J. *J. Am. Chem. Soc.* **1968**, *90*, 1499.

(9) Wei, H.; Hrovat, D. A.; Borden, W. T. *J. Am. Chem. Soc.* **2006**, *128*, 16676.

(10) Wei, H.; Hrovat, D. A.; Dolbier, W. R., Jr.; Smart, B. E.; Borden, W. T. *Angew. Chem., Int. Ed.* **2007**, *46*, 2666.

(11) Reviews: (a) Hoffmann, R. *Acc. Chem. Res.* **1971**, *4*, 1. (b) Gleiter, R. *Angew. Chem. Int Ed.* **1974**, *13*, 696. (c) Paddon-Row, M. N. *Acc. Chem. Res.* **1982**, *15*, 245. (d) Gleiter, R.; Schäfer, W. *Acc. Chem. Res.* **1990**, *23*, 369.

(12) For recent reviews of VB theory, see: (a) Shaik, S.; Shurki, A.; Danovich, D.; Hiberty, P. C. *Chem. Rev.* **2001**, *101*, 1501–1539. (b) Shaik,

S.; Hiberty, P. C. *A Chemist's Guide to Valence Bond Theory*; Wiley-Interscience: New York, 2007.

(13) Song, L. C.; Mo, Y. R.; Zhang, Q.; Wu, W. *J. Comput. Chem.* **2005**, *26*, 514.

(14) (a) Review: Goddard, W. A., III; Dunning, T. H.; Hunt, W. J.; Hay, P. J. *Acc. Chem. Res.* **1973**, *6*, 368.

(15) Gaussian 03, Revision D.02, Frisch, M. J. et al., Gaussian, Inc., Wallingford CT, 2004. The full list of authors is given in the Supporting Information.

(16) Review: Borden, W. T. In *Diradicals*; Borden, W. T., Ed.; Wiley-Interscience: New York, 1982; pp. 1–72.

(17) This information is available free of charge via the Internet at http://pubs.acs.org. See any current masthead page for ordering information and Web access instructions.

(18) We are indebted to Professor Wei Wu for providing us with his program.

(19) Hariharan, P. C.; Pople, J. A. *Theor. Chim. Acta.* **1973**, *28*, 213.

(20) (a) Anderson, K.; Malmqvist, P. A.; Roos, B. O. *J. Chem. Phys.* **1992**, *96*, 1218. (b) Andersson, K.; Malmqvist, P. A.; Roos, B. O.; Sadlej, A. J.; Wolinski, K. *J. Chem. Phys.* **1990**, *94*, 5483.

(21) Molcas Version 6.4 Karlström, G.; Lindh, R.; Malmqvist, P.-Å; Roos, B. O.; Ryde, U.; Veryazov, V.; Widmark, P.-O.; Cossi, M.; Schimmelpfennig, B.; Neogrady, P.; Seijo, L. *Comput. Mater. Sci.* **2003**, *28*, 222.

(22) If the pair of electrons that form the C(1)—C(3) bond are localized, one at C(1) and the other at C(3), and if the energies of the resulting singlet and triplet VB wave functions are averaged, the energy of the quasi-classical state that results is equal to the energy of a hypothetical diradical in which there is no TS interaction between the electrons localized at C(1) and C(3).[12b] At the ROHF geometry of the triplet, the energy of this hypothetical diradical is 1.9 kcal/mol below the VB energy of the triplet and 8.5 kcal/mol above the VB energy of the singlet, when the latter is computed at the GVB optimized geometry.

(23) At least at the GVB/ROHF level of theory, basis set seems to have little effect on the calculated values of ΔE_{S-T}. See footnote e of Table 1.

(24) Reviews: (a) Hiberty, P. C. In *Modern Electronic Structure Theory and Applications in Organic Chemistry*; Davidson, E. R., Ed.; World Scientific: River Edge, NJ., 1997; pp. 289–367. (b) Hiberty, P. C.; Shaik, S. *Theor. Chem. Acc.* **2002**, *108*, 255.

(25) See, for example, refs 5a, b, e, h, i, l, n, p, q.

(26) On bending of a linear, first-row AH$_2$ molecule, the nonbonding 2p AO on A that lies in the molecular plane interacts most strongly with the $3\sigma_g$ MO of the linear molecule. The $3\sigma_g$ MO is the antibonding combination of the valence 2s orbital on A with the in-phase combination of the two hydrogens. Mixing between the nonbonding 2p AO on A and $3\sigma_g$ stabilizes this 2p AO and transforms it into the $3a_1$ MO of the bent AH$_2$ molecule. As shown in Figure 5b for ^{3}CH$_2$, in this MO, the AO on A is hybridized away from the hydrogens, but the smaller lobe of the hybridized AO on A interacts in a bonding fashion with the 1s AOs of H. For more pictures and detailed descriptions, see, for example, (a) Borden, W. T. *Modern Molecular Orbital Theory for Organic Chemists*; Prentice-Hall: Englewood Cliffs, NJ, 1975; pp. 34–38. (b) Cherry, W.; Epiotis, N.; Borden, W. T. *Acc. Chem. Res.* **1977**, *10*, 167. (c) Albright, T. A.; Burdett, J. K.; Whangbo, M. H. *Orbital Interactions in Chemistry*; Wiley-Interscience: New York, 1985; pp. 87–97.

(27) The 2p AO at C(1) of **6** mixes with appropriate symmetry combinations of both the bonding and antibonding orbitals that are associated with the bonds to C(2). In the SOMO of **6**, the bonding orbitals at C(2) are mixed with the 2p AO on C(1) in an antibonding fashion, whereas the antibonding orbitals at C(2) are mixed with the 2p AO in a bonding fashion. The net results of the mixing of the 2p AO at C(1) with the bonds to C(2) are two-fold: (a) the contributions of the AOs on C(2) tend to cancel in the SOMO, whereas (b) the AOs on the distal atoms that contribute to these bonds add and are mixed into the SOMO with a phase opposite to that of the 2p AO. The same considerations explain how the interaction of the 2p AO on C(1) in planar allyl radical with the π and π^* orbitals of the π bond between C(2) and C(3) gives rise to the SOMO, which has a node at C(2) and opposite phases at C(1) and C(3).

(28) In eq 10, replace $c_3\phi_1$ and $c_3\phi_3$ with $c_3\phi_1'$ and $c_3\phi_3'$, where the primed AOs are the rotated distal AOs that contribute to the GVB orbitals. The resultant AOs at C(1) and C(3) then become, respectively, $\phi_1 \pm (c_3/c_1)\phi_1'$ and $\phi_3 \pm (c_3/c_1)\phi_3'$, where the positive signs are for the AOs in Ψ_S and the negative signs are for the AOs in Ψ_A.

(29) As R_{13} decreases, TB interactions also stabilize Ψ_A', because the antibonding interaction between the radially oriented 2p AO on C2 and the large lobes of the AOs on C(1) and C(3) decreases in C(1)—C(2)—C(3) decreases. Nevertheless, at least down to $R_{13} = 1.800$ Å, the increase in stabilizing TB interactions with decreasing R_{13} is greater for Ψ_S' than for Ψ_A'. Therefore, with decreasing values of R_{13}, TB interactions contribute to increasing not only the adiabatic but also the vertical values of ΔE_{S-T}(GVB/ROHF).

(30) If fluorine, rather than hydrogen, is attached to C(2), the low-lying C—F σ^* orbital can mix with Ψ_S and thus provides net stabilization for this MO. (Review: Borden, W. T. *Chem. Commun.* **1998**, 1919). In fact, we calculate ΔE_{S-T}(GVB/ROHF) = 15.3 kcal/mol at the TCSCF optimized geometry of 2-fluoro-1,3-dehydrobenzene, which is 2.6 kcal/mol (20%) larger than the value in unsubstituted **1**. However, only 1.5 kcal/mol of this increase comes from the larger increase in ^1E(TB) (1.9 kcal/mol) than in ^3E(TB) (0.4 kcal/mol) on substitution of fluorine for

hydrogen at C(2) of **1**. The remaining 1.1 kcal/mol increase in ΔE_{S-T}(GVB/ROHF) comes from ΔE_{S-T}(TS) and is, presumably, due to the small, but visible, spatial reorientation of the AOs at C(1) and C(3) upon substitution of the more electronegative fluorine for hydrogen at C(2).

JP905222F